

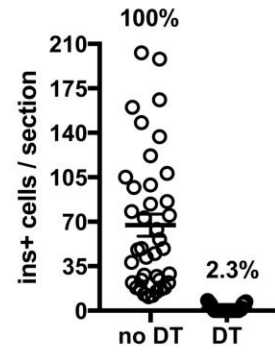
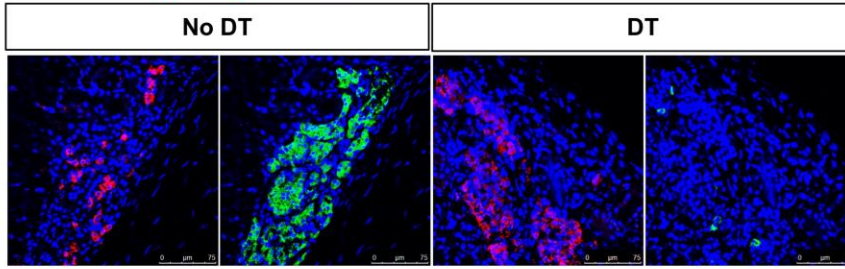
In the format provided by the authors and unedited.

Pancreatic islet-autonomous insulin and smoothed-mediated signalling modulate identity changes of glucagon⁺ α -cells

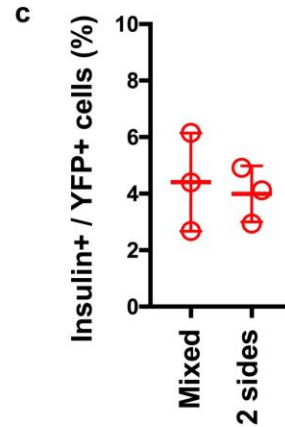
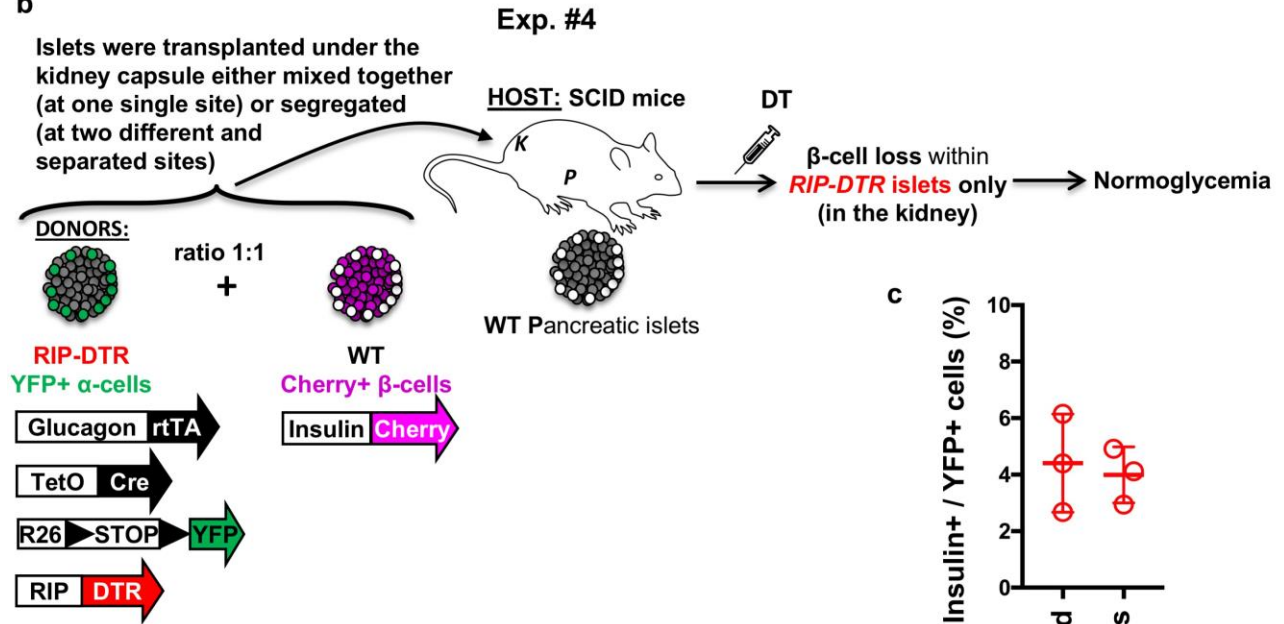
Valentina Cigliola^{1,2,10}, Luiza Ghila ^{1,3,10}, Fabrizio Thorel^{1,10}, Léon van Gurp¹, Delphine Baronnier¹, Daniel Oropeza¹, Simone Gupta⁴, Takeshi Miyatsuka⁵, Hideaki Kaneto⁶, Mark A. Magnuson ⁷, Anna B. Osipovich⁷, Maike Sander⁸, Christopher E. V. Wright⁹, Melissa K. Thomas⁴, Kenichiro Furuyama¹, Simona Chera^{1,3} and Pedro L. Herrera ^{1*}

¹Department of Genetic Medicine and Development, iGE3 and Centre facultaire du diabète, Faculty of Medicine, University of Geneva, Geneva, Switzerland. ²Present address: Department of Cell Biology, Duke University Medical Center, Durham, NC, USA. ³Department of Clinical Science and KG Jebsen Center for Diabetes Research, University of Bergen, Bergen, Norway. ⁴Lilly Research Laboratories, Lilly Corporate Center, Indianapolis, IN, USA. ⁵Department of Metabolism and Endocrinology, Graduate School of Medicine, Juntendo University, Tokyo, Japan. ⁶Department of Metabolic Medicine, Graduate School of Medicine, Osaka University, Osaka, Japan. ⁷Departments of Molecular Physiology and Biophysics, Center for Stem Cell Biology, Vanderbilt University, Nashville, TN, USA. ⁸Department of Pediatrics and Cellular and Molecular Medicine, University of California, San Diego, CA, USA. ⁹Department of Cell and Developmental Biology, Program in Developmental Biology and Center for Stem Cell Biology, Vanderbilt University School of Medicine, Nashville, TN, USA. ¹⁰These authors contributed equally: Valentina Cigliola, Luiza Ghila, Fabrizio Thorel. *e-mail: pedro.herrera@unige.ch

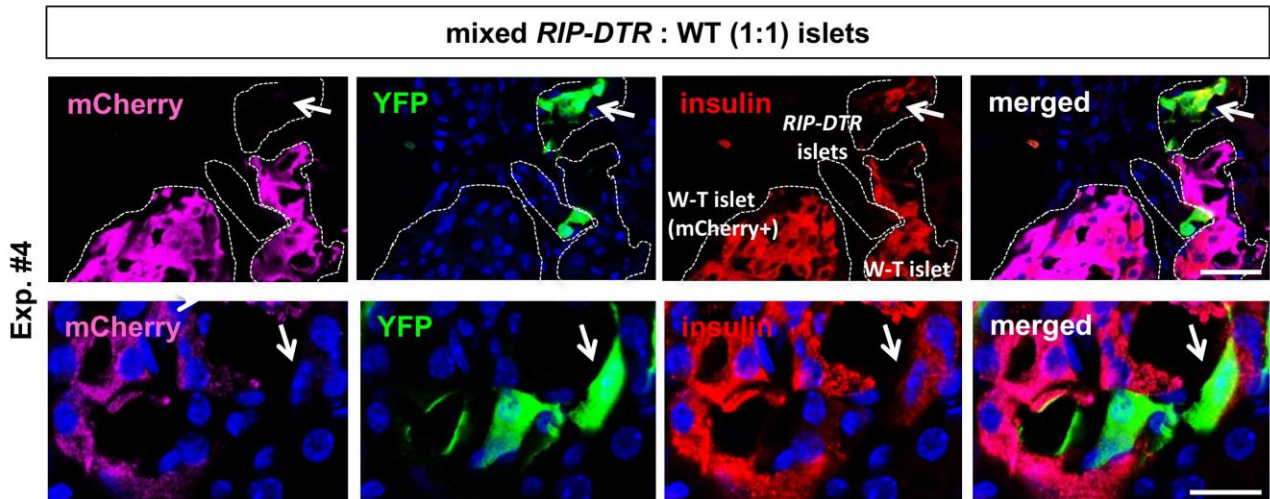
a Kidney; glucagon Insulin



b



d

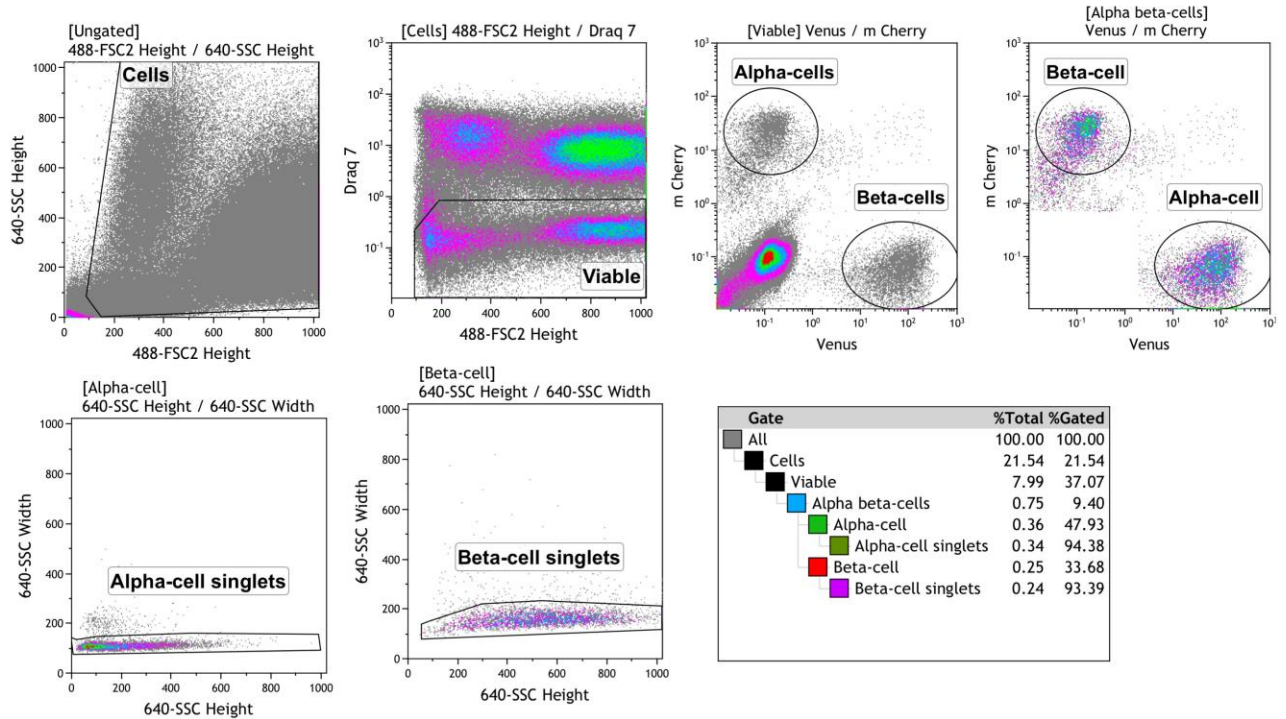


Supplementary Figure 1

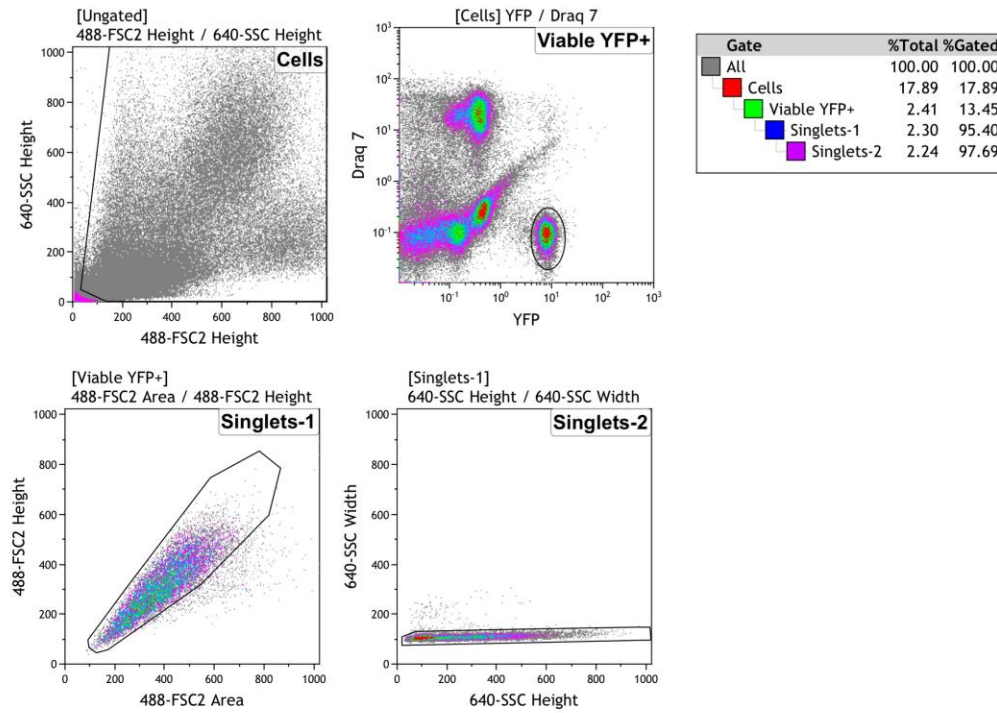
Insulin production by α -cells after β -cell ablation in islets transplanted under the kidney capsule.

(a) Immunofluorescence staining of insulin (green) and glucagon (red) in *RIP-DTR* islets transplanted under the kidney capsule, either before (“no DT”) or after (“DT”) β -cell ablation. The scatter graph reports a quantification of the β -cell ablation efficiency, measured as the number of insulin-containing cells remaining per islet section in non-treated and DT-treated animals, 10 days later. (mean \pm s.e.m., n=40 islet sections per condition. **(b)** Experimental design of Exp. #4, where islets were transplanted in the kidney capsule of immunocompromised mice (SCID) either mixed together or at 2 separated sites. **(c)** Proportion of YFP-traced α -cells expressing insulin 1-month post-DT in mixed *RIP-DTR*+WT islets compared to *RIP-DTR* islets from 2-sides graft. Data are shown as mean \pm s.d.; n=3 biologically independent animals per condition. **(d)** Immunofluorescence staining of mCherry (magenta), YFP (green), insulin (red) in transplanted mixed *RIP-DTR*+WT islets 1-month post-DT. Scale bars: 20 μ m. Experiment repeated independently 3 times. See Supplementary Table 1 as source data.

α- and β- cell sorting from Gcg-Venus / RIP-mCherry transgenic mice.



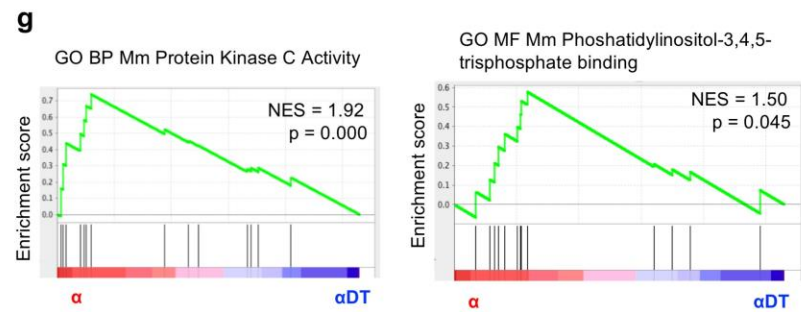
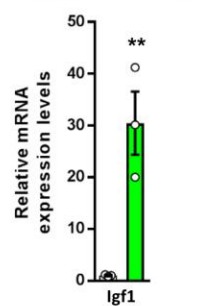
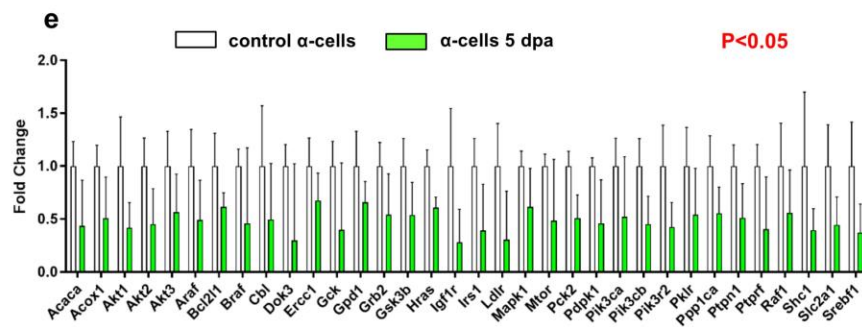
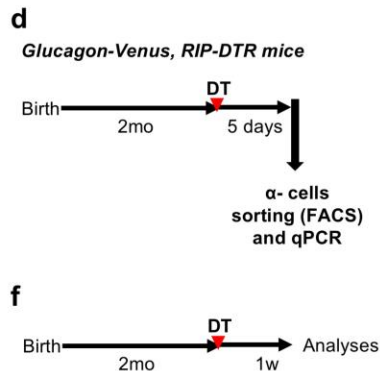
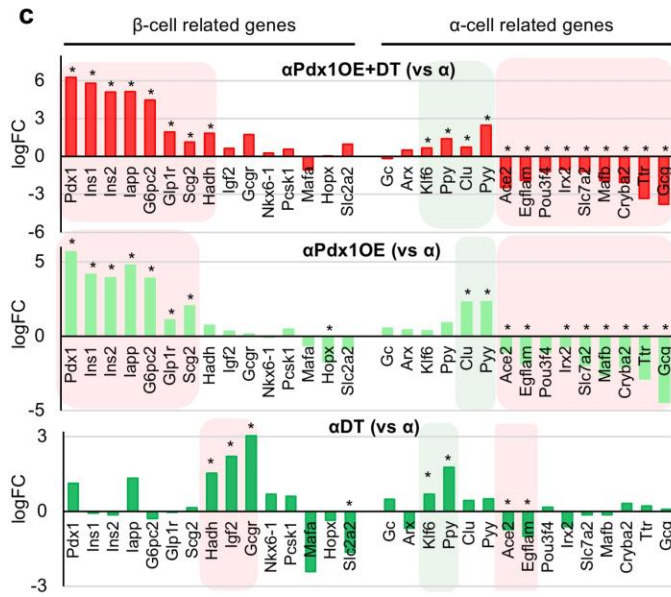
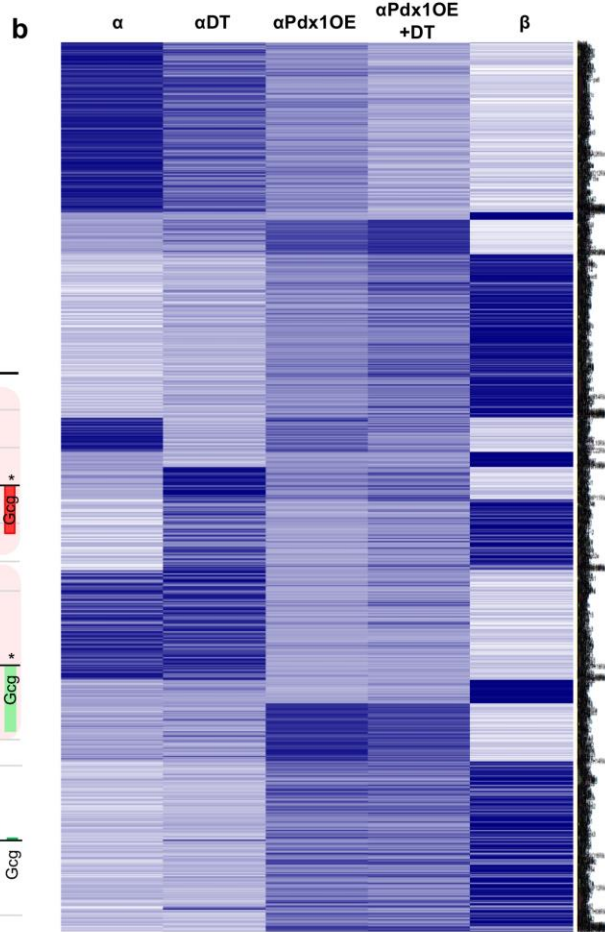
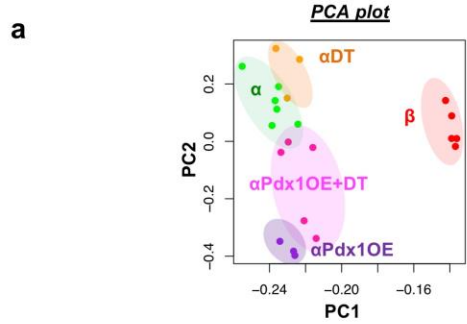
α-cell sorting from transgenic mice allowing Gcg⁺ cell-lineage tracing through DOX administration.



Supplementary Figure 2

FACS sorting.

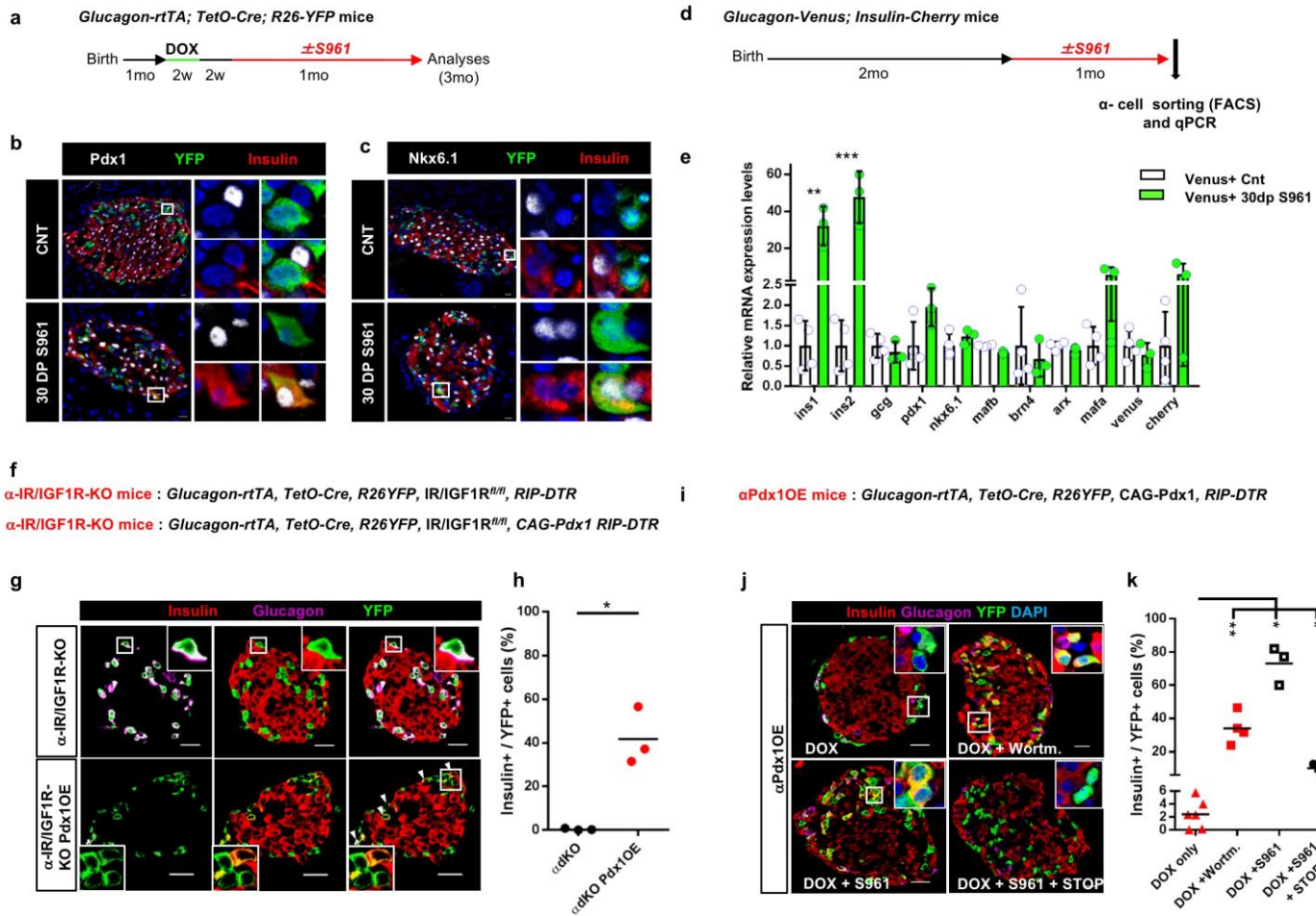
Gating strategy used for FACS sorting the different islet cell types used for RNA seq analyses. Mice used to purify the different islet cell types are listed in the methods.



Supplementary Figure 3

α -cell transcriptome analysis and gene expression changes after β -cell loss.

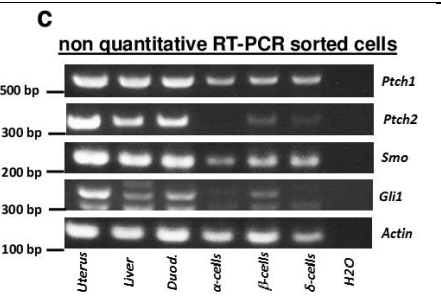
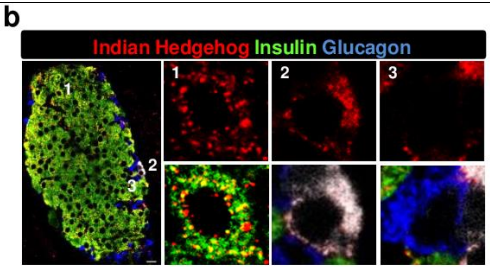
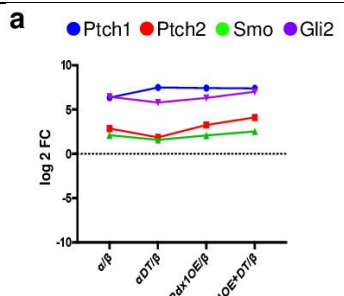
(a) PCA plot of all samples analyzed by RNA-Seq. Native β -cells (" β ", n=5 mice) show a different profile compared to α -cell groups including native α -cells (" α ", n=6 mice), α -cells 1 month after DT-induced β -cell ablation (" α DT", n=3 mice), α -cells overexpressing Pdx1 (" α Pdx1OE", n=3 mice), and α -cells overexpressing Pdx1 combined with β -cell ablation (" α Pdx1OE+DT", n=5 mice). **(b)** Heat map showing scaled expression (blue, high; white, low) of α - / β -cell-enriched genes differentially expressed in α DT, α Pdx1OE, α Pdx1OE+DT conditions compared to native α -cells. **(c)** Gene expression changes (log2 value) in α Pdx1OE+DT (top), α Pdx1OE (middle) and α DT (bottom) compared to native α -cells. DEGs indicated by red-colored background show induced β -cell signature upon the conditions, while DEGs indicated by green-colored background show refractory responses. * FDR < 0.05. n = 6 mice in α , n = 5 mice in α Pdx1OE+DT, n = 3 mice in α Pdx1OE, and n = 3 mice in α DT. **(d)** Transgenes required for constitutive labeling α -cells with the reporter *Venus* and experimental design for α -cell labeling and purification after β -cell loss. **(e)** RT-qPCR analyses for different components of the insulin/IGF1-R signaling pathway. Components of the pathway are downregulated in α -cells 5 days post-DT. Center indicates the mean. qPCR were performed in triplicates and data processing and statistical analyses were performed using the web-based software "RT2 Profiler PCR Array Data Analysis version 3.5", from Qiagen. Quantification of the gene expression changes were performed using the $2^{-\Delta\Delta Ct}$ method. *P*-values were calculated using a Student's t-test (two-tail distribution and equal variances between the two samples) on the $2^{-\Delta Ct}$ values. Genes with *P*<0.05 are shown. n=3 mice. qPCR was performed once. **(f)** Experimental design for DT-mediated β -cell loss, islet isolation and qPCR. *Igf1* mRNA is upregulated in islets after β -cell loss, likely as an attempt to sustain insulin signaling. Data shown as mean \pm sem; n=3 mice with 3 technical replicates each. Center indicates the mean. Two-tailed unpaired t-test *P*=0.0086. **(g)** Gene set enrichment analysis (GSEA) from RNA-Seq showing enrichment of the insulin signaling pathway components PKC (left) and PI3K (right) in α -cells after DT-mediated β -cell ablation (α DT) compared to native α -cells (α). *P*-values were calculated by an empirical phenotype-based permutation test. n = 6 mice in α , n = 3 mice in α DT. NES: normalized enrichment score. See Supplementary Table 2 as source data.



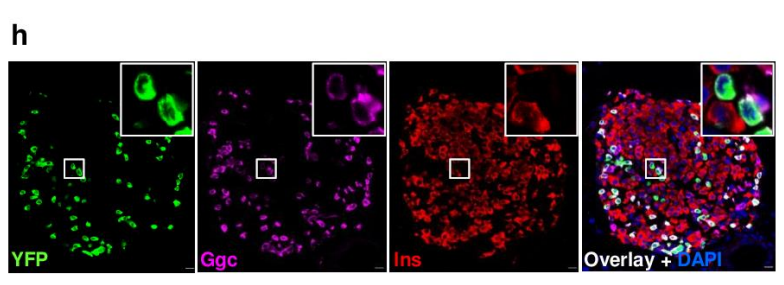
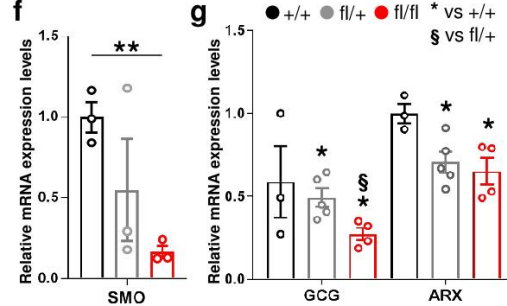
Supplementary Figure 4

Insulin production in α-cells under insulin signaling blockade.

(a) Transgenes for inducible α-cell lineage tracing and experimental design for α-cell lineage tracing and S961 treatment. **(b-c)** Immunofluorescence staining for the β-cell-specific transcription factors Pdx1 and Nkx6.1 in islets of mice treated for 1 month with S961. Experiments were repeated once, with $n=3$ mice treated asynchronously according to their availability. **(d)** Mice and experimental design for α-cell labeling and sorting by FACS. **(e)** β-cell-specific genes are upregulated in α-cells upon S961 treatment. qPCRs were performed in triplicates. Data shown as mean \pm sem; $n=3$ mice. Experiment performed once. Two-tailed unpaired t-test ($P=0.0017$ INS1; $P=0.0010$ INS2) **(f)** Transgenes required for inducible α-cell lineage tracing, simultaneous insulin receptor (IR) and IGF-1 receptor (IGF1R) downregulation, and ectopic Pdx1 induction in adult α-cells. **(g)** Impaired insulin/IGF1 signaling in α-cells through IR and IGF1R downregulation predisposes α-cells to insulin gene expression in mice with normal β-cell mass. **(h)** Fractions of α-cells expressing insulin after IR/IGF1R downregulation in α-cells and Pdx1OE. $n = 3$ mice. Two-tailed Mann Whitney test, $P=0.05$. **(i)** Transgenes required for inducible Pdx1 expression in adult α-cells. **(j)** Wortmannin-mediated PI3K inhibition or S961-mediated insulin antagonism trigger insulin production in Pdx1OE α-cells. Insulin production in Pdx1OE α-cells is reversed when islets are analyzed 1 month after ending S961 treatment. **(k)** Fraction of converted α-cells found upon insulin signaling antagonism/inhibition. Black and red symbols: control and αPdx1OE mice, respectively. $n = 6, 4, 3, 3$ mice in DOX only, DOX+Wort, DOX+S961 and DOX+S961+STOP, respectively. Two-tailed Mann Whitney test, $P=0.0061$ Pdx1 only vs Pdx1+wort, $P= 0.0167$ Pdx1 only vs Pdx1+S961, $P= 0.0333$ Pdx1 only vs Pdx1+S961then stop. All experiments were performed once with animals treated in an asynchronous way depending on their availability. Scale bars: 20 μ m. See Supplementary Table 1d as source data.

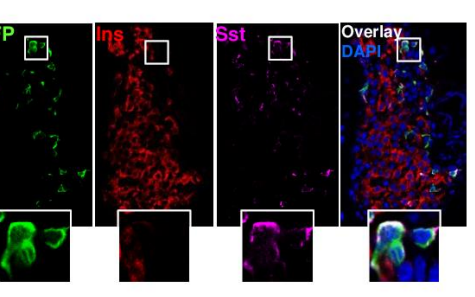
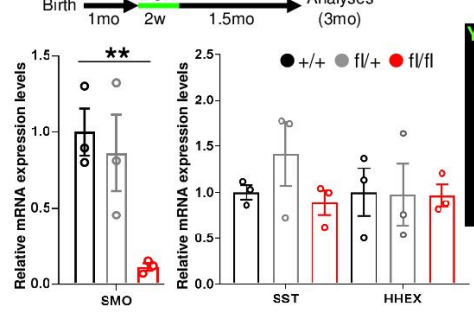
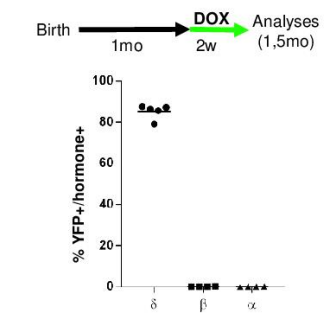


d α-Smo-KO mice : Glucagon-rtTA, TetO-Cre, R26YFP, Smoothened^{fl/fl}, RIP-DTR



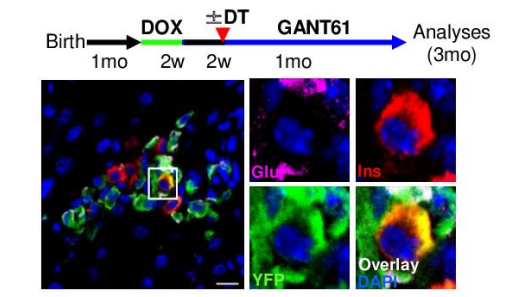
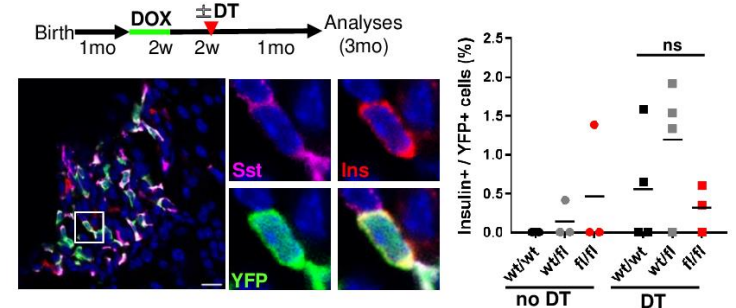
j Somatostatin-rtTA, TetO-Cre R26YFP mice

k δ-Smo-KO mice : Somatostatin-rtTA, TetO-Cre, R26YFP, Smoothened^{fl/fl}, RIP-DTR



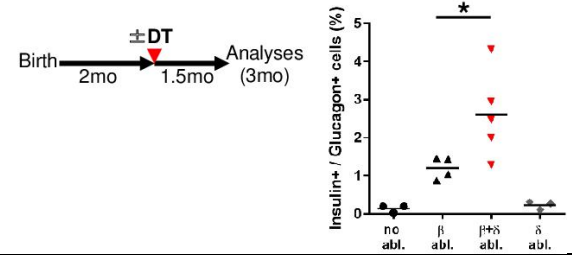
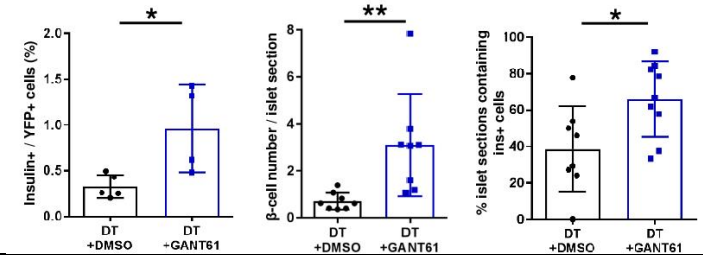
k δ-Smo-KO mice : Sst-rtTA, TetO-Cre, R26YFP, Smoothened^{fl/fl}, RIP-DTR

l Glucagon-rtTA, TetO-Cre, R26YFP, RIP-DTR



m Glucagon-rtTA, TetO-Cre, R26YFP, RIP-DTR

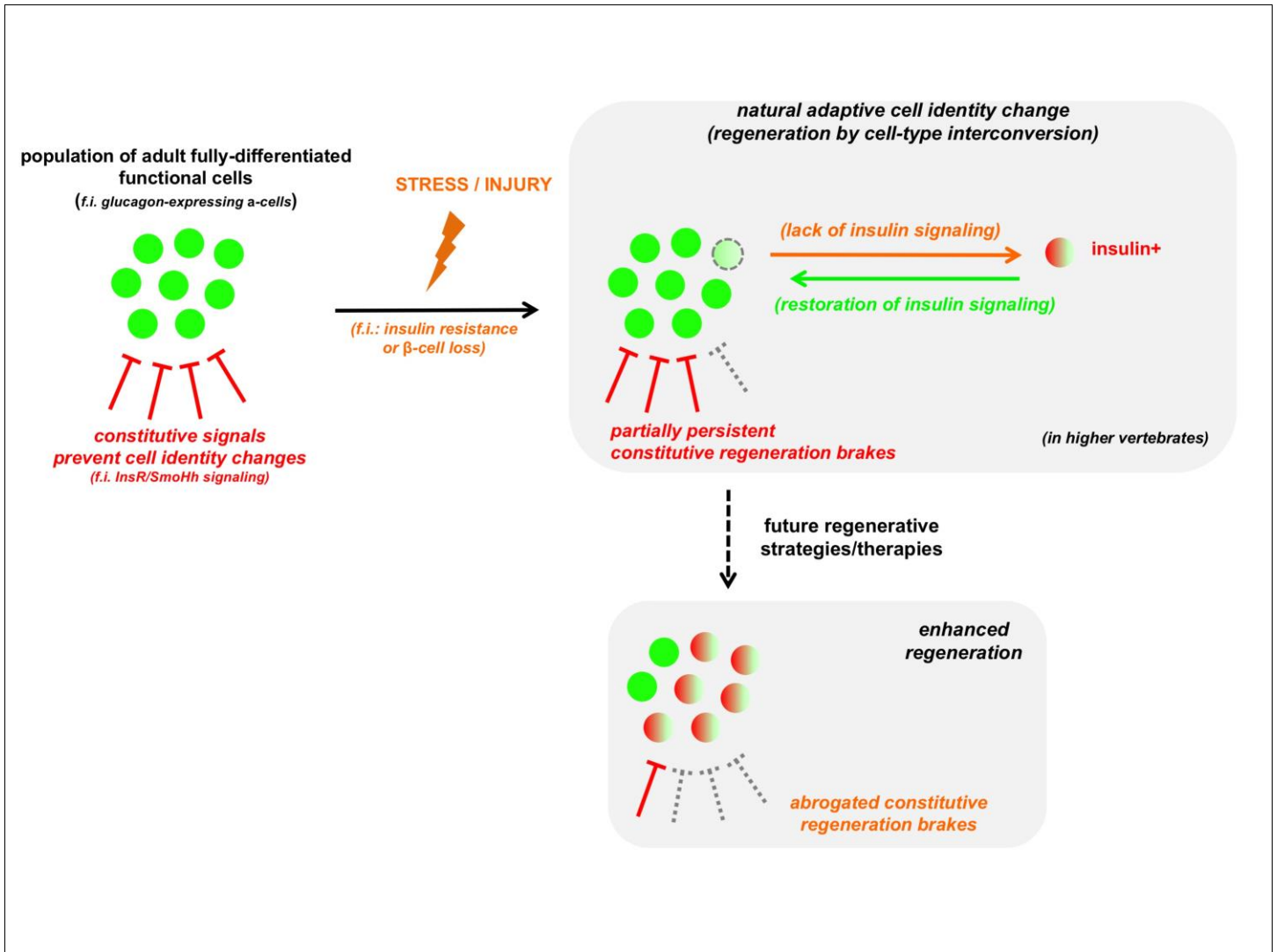
n Somatostatin-Cre, R26YFP, R26-DTR, RIP-DTR



Supplementary Figure 5

Hedgehog signaling modulation in α - and δ -cells.

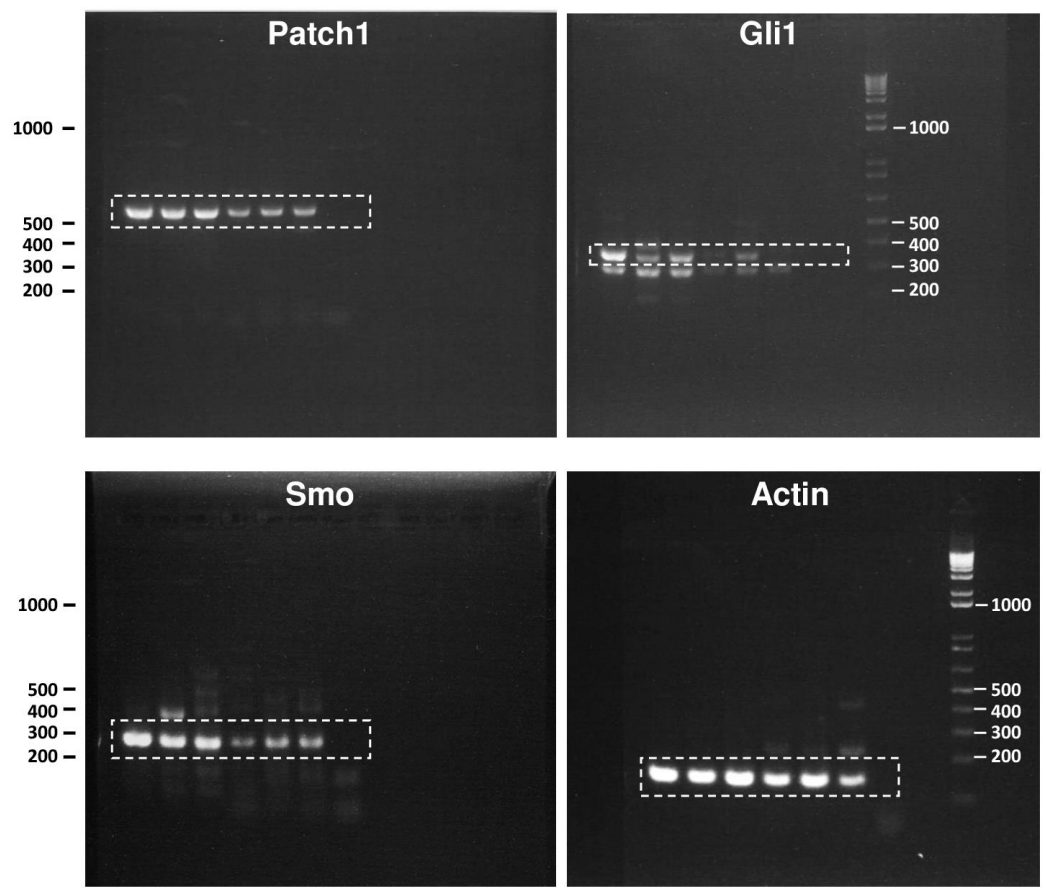
(a) Hh signaling components are enriched in α - vs β -cells and their expression is unchanged 30 days upon DT-induced β -cell ablation, Pdx1OE or both. Log2FC are taken from the RNA-Seq presented in Fig.3. **(b)** Indian Hedgehog ligand expression in islets of control mice. Immunofluorescence was repeated two times with similar results. **(c)** Non-quantitative RT-PCR of Hedgehog pathway's components in sorted α -, δ - and β -cells. Liver, duodenum and uterus were used as controls. Experiments were repeated three times with similar results. Unprocessed scans of the blots are provided in Suppl. Fig.7. **(d)** Transgenes required for simultaneous α -cell lineage tracing, *Smo* co-receptor downregulation and DT-induced β -cell ablation. **(e)** Experimental design. **(f)** *Smo* and **(g)** α -cell genes *Arx* and *Glucagon* are downregulated in α -cells with reduced *Smo* activity upon DOX treatment. $n=3$ mice. qPCR was performed once. Two-tailed unpaired t-test; SMO: $P=0.0012$, GCG: $P=0.0325$ $fl/+$ vs $+/+$ $P=0.0141$ fl/fl vs $+/+$ and $P=0.0177$ fl/fl vs $fl/+$, ARX: $P=0.0214$ $fl/+$ vs $+/+$, 0.0245 fl/fl vs $+/+$). Center indicates the mean. **(h)** *Smo* inactivation in α -cells in absence of β -cell loss or insulin signaling impairment does not lead to insulin production in intact islets. Immunofluorescence was repeated once, on 2 slides of 3 different mice. **(i)** Transgenes required to lineage trace δ -cells, experimental design and characterization of labeling specificity in the *Sst-rtTA* line. Only δ -cells express YFP. $n = 5, 4, 4$ for δ -, β - and α -cells, respectively. **(j)** Transgenes required for lineage tracing and *Smo* coreceptor inactivation in δ -cells, and for DT-induced β -cell ablation and experimental design. *Smo* is downregulated in purified δ -cells after DOX treatment. $n=3$ mice. qPCRs were performed once. Two-tailed unpaired t-test, $P=0.0048$. Downregulation of *Smo* in δ -cells does not alter the expression of the δ -cell genes *Somatostatin* and *Hhex*. $n=3$ mice. qPCR was performed once. Center indicates the mean. Insulin protein is not expressed in δ -cells upon *Smo* inactivation in intact islets. Immunofluorescence was repeated once, on 3 slides of 3 different mice. **(k)** Experimental design for δ -cell lineage tracing and DT-induced β -cell loss in δ -*Smo*-KO mice. A fraction of δ -cells express insulin after β -cell ablation in δ -*Smo*-KO mice, but their percentage is not increased when compared to mice with intact *Smo* expression. $n = 3, 3, 3$ mice in no DT wt/wt , wt/fl , fl/fl respectively and $n = 4, 4, 3$ mice in DT wt/wt , wt/fl , fl/fl respectively. Immunofluorescence was repeated once, on 3 to 5 slides per mouse. Center in the graph indicates the mean. Two-tailed unpaired t-test. **(l)** Transgenes required for α -cell tracing and DT-induced β -cell ablation, experimental design and immunofluorescence staining of mouse islets 1 month after DT+GANT61 treatment. Immunofluorescence was repeated once, on 3 to 5 slides of $n = 8$ mice treated with DT+GANT61. A representative islet is shown. **(m)** The % of α -cells expressing insulin ($n = 5$ and 4 mice for DT+DMSO and DT+GANT61, respectively), the number of insulin-expressing cells per islet section ($n = 8$ mice for DT+DMSO and DT+GANT61), and the % of islets containing insulin⁺ cells ($n = 8$ mice and $n=9$ mice for DT+DMSO and DT+GANT61, respectively) are increased in mice treated with GANT61 after DT-induced β -cell loss. Two-tailed unpaired t-test ($P=0.0236$ panel left, $P=0.0085$ middle, $P=0.0213$ right graph). **(n)** Transgenes required for simultaneous β - and δ -cell ablation, experimental design and percentage of cells coexpressing insulin and glucagon after β - and δ -cell loss. $n = 4, 5, 3$ mice for β -, $\beta+\delta$ and δ -cell ablation, respectively. Center indicates the mean. Two-tailed unpaired t-test, $P=0.0494$. Scale bars: 10 μ m. See Supplementary Table 1m,n,q as source data.



Supplementary Figure 6

Constitutive signals ensure maintenance of cell identity.

In physiological conditions, the identity of fully differentiated cells (such as α -cells) is maintained through a variety of constitutive signals preventing cell identity changes. Most of these brakes (f.i. insulin signaling) are preserved upon stress and injury (f.i. β -cell loss). However, few cells may undergo changes in cell identity as an attempt to replenish the compromised cell population (f.i. α -cells produce insulin to cope with insulin insufficiency). Due to the persistence of most constitutive brakes, this kind of natural cell interconversion events are rare and help explaining the poor regenerative capacity observed in higher vertebrates. Insulin-expressing α -cells may reacquire their initial fate upon restoration of physiological conditions (reversibility). Future therapies aimed at identifying and abrogating constitutive regeneration brakes should improve the intrinsic regenerative capacity of likely any organ.



Supplementary Figure 7

Unprocessed blots.

Unprocessed scans of the non-quantitative PCR blots provided in Supplementary Fig. 6.

Supplementary Table 1. Statistics Source Data.

a) Statistics Source Data for for Figure 1 and Supplementary Figure 1

Proportion of α -cells that engage in insulin expression after β -cell ablation in islets transplanted under the kidney capsule of SCID host mice.

b) Statistics Source Data for Figure 2

Percentage of YFP+ α -cells expressing glucagon or insulin in control and α Pdx1OE mice in presence of intact β -cell mass.

c) Statistics Source Data for for Figure 2

Pancreatic content in control and α Pdx1OE mice.

d) Statistics Source Data for Fig.2 and Supplementary Figure 4

Conversion rate of YFP-labeled α -cells to insulin production in Pdx1OE mice.

e) Statistics Source Data for Figure 4

Conversion rate of YFP-labeled α -cells to insulin production after insulin signaling blockade and administration of insulin pellets.

f) Statistics Source Data for Figure 5

Conversion rate of YFP-labeled α -cells to insulin production in α -Smo-KO mice.

g) Statistics Source Data for Supplementary Fig.5

In vivo GSIS (1 month after DT in α -Smo-KO mice).

h) Statistics Source Data for Supplementary Fig.5

α -cells FACS-sorting from Smo-KO mice for pseudoislets reconstruction.

i) Statistics Source Data for Supplementary Fig.5

% of Smo-KO α -cells producing insulin in pseudoislets.

l) Statistics Source Data for Supplementary Fig.5

In vitro GSIS of composed of Smo-KO α -cell pseudoislets.

m) Statistics Source Data Supplementary Figure 5

Labeling of δ -, β - and α -cells in the Somatostatin-rtTA mouse line.

n) Statistics Source Data for Figure 6 and Supplementary Figure 6

Conversion rate of YFP-labeled δ -cells to insulin production in δ -Smo-KO mice.

o) Statistics Source Data for Figure 6

% of cells coexpressing glucagon and insulin in δ -Smo-KO mice.

p) Statistics Source Data for Figure 6

Conversion rate of YFP-labeled α -cells to insulin production in α + δ -Smo-KO mice.

q) Statistics Source Data for Supplementary Figure 6

Cells coexpressing glucagon and insulin after β -, δ + β - and δ -cell ablation.

Supplementary Table 2: RNA analyses

- DEGs between α - vs β -cells at a fold change (FC) >2 ($\log_2\text{FC} > 1$) and false discovery rate (FDR) <0.01 .
- Data of all comparisons in α DT, α Pdx1OE and α Pdx1OE+DT compared to native α -cells.
- DEG lists in α -Pdx1OE (vs α)
- DEG lists in α DT (vs α)
- DEG lists in α Pdx1OE+DT (vs α)
- Gene lists in Venn diagram shown in Fig. 2d
- Gene set list significantly modulated upon DT-induced β -cell loss in α -cells (related to GSEA in Suppl. Fig. 6f)

Supplementary Table 3: Primers

List of primers used for qPCR analyses.

Supplementary Table 4: Antibodies

List of antibodies used for Immunofluorescence.